IUST
Iran University of Science and Technology

Iranian Journal of Electrical and Electronic Engineering

Journal Homepage: ijeee.iust.ac.ir

Advanced Photovoltaic Emulator with ANN-Based Modeling Using a DC-DC Push-Pull Converter and LQR Control with Current Observer

A. Hadjaissa*(C.A.), M. Benmiloud*, K. Ameur*, H. Bouchnak** and M. Dimeh**

Abstract: As solar photovoltaic power generation becomes increasingly widespread, the need for photovoltaic emulators (PVEs) for testing and comparing control strategies, such as Maximum Power Point Tracking (MPPT), is growing. PVEs allow for consistent testing by accurately simulating the behavior of PV panels, free from external influences like irradiance and temperature variations. This study focuses on developing a PVE model using deep learning techniques, specifically a Multi-Layer Perceptron (MLP) Artificial Neural Network (ANN) with backpropagation as the learning algorithm. The ANN is integrated with a DC-DC push-pull converter controlled via a Linear Quadratic Regulator (LQR) strategy. The ANN emulates the nonlinear characteristics of PV panels, generating precise reference currents. Additionally, the use of a single voltage sensor paired with a current observer enhances control signal accuracy and reduces the PVE system's hardware requirements. Comparative analysis demonstrates that the proposed LQR-based controller significantly outperforms conventional PID controllers in both steady-state error and response time.

Keywords: Photovoltaic Emulators (PVEs), Artificial Neural Network (ANN), DC-DC Push-Pull Converter, LQR Strategy, Luenberger Observer.

1 Introduction

THE global transition to renewable energy is accelerating as countries and industries increasingly commit to reducing their carbon footprints and mitigating climate change. In 2024, total renewable energy production reached 8,439.6 terawatts (TW) [1]. Of this production, the deployment of photovoltaic (PV) sources is expected to continue its rapid growth, with global solar PV installations projected to reach 462 gigawatts of direct current (GWdc), representing a 17% increase from 2023 [2].

This growth has led to extensive research on solar PV systems, which aims to enhance the systems' efficiency, performance, and robustness [3],[4].

One crucial issue of a PV power generator is its control algorithm, maximum power point tracking, which extract the maximum power from the PV module despite variations in load or environmental conditions. The laboratory testing and validation of PV panels must be conducted under standard test conditions (STC). However, these tests are complex, inflexible, and require careful manipulation of temperature and light sources. Additionally, it could be more efficient, demanding high power to produce the necessary irradiance. The PVE is an alternative setup for MPPT algorithm testing, which offers a more streamlined and efficient approach [5],[6]. A PVE system functions as a programmable DC source designed to replicate the electrical output characteristics of various PV panels, irrespective of external atmospheric conditions. The PVE's capability enables precise validation of MPPT techniques applied in PV systems, accommodating both uniform and partial shading conditions. The PVE provides convenient control over ambient conditions for transient responses

Iranian Journal of Electrical & Electronic Engineering, 2024.
Paper first received 07 August 2024 and accepted 22 October 2024.
* The authors are with the LACoSERE Laboratory, University of Laghouat, Algeria.
E-mail: b.hadjaissa@lagh-univ.dz.
** The authors are with the Department of Electronics, University of Laghouat, Algeria.
Corresponding Author: Aboubakeur Hadjaissa.

and steady-state error, facilitating rapid, and precise experiments and tests for PV power systems [7],[8],[9].

In research studies on PVEs, the development typically focuses on three main axes: the power converter used, the control strategy employed, and the PV model itself. In the sequel, we address each component's a brief state of the art.

1.1 Part 1: Power converter

Various power converters are employed in PV emulators to generate power for the load. These converters fall into three categories [5]: linear regulators [10], switched-mode power supplies [5],[6],11], and programmable power supplies [12]. The most commonly used are switched-mode power supplies, over other types of converters due to their higher efficiency, compact size, lighter weight, wide input voltage range, less heat generation, better voltage regulation, scalability, higher power density, and easy control of the output voltage/ current. Additionally, various topologies are utilized in PVEs within this category [5], including boost converters, buck converters [13], Z-source converters, flyback converters [14], interleaved buck converters [15], and push-pull converters [6],[16].

1.2 Part 2: Control Strategy

The control strategy of the PVE is designed to enforce the operating point generated by the PV model (current/voltage) by minimizing the error between the measured value and the reference set by the PV model, which effectively replicates the output impedance of the PV panel. In the literature, numerous strategies for controlling PVEs have been discussed [5]. We note Hybrid-Mode controlled strategy [17], Perturb and observe strategy [18], resistance comparison strategy [19], analog-based control strategy [20] and include direct referencing methods [6],[21],[22],[23]. The latter strategy is widely used due to its simplicity and is applicable in both closed-loop current mode and closed-loop voltage mode control. These strategies employ well-known controllers such as PID, LQR, fuzzy logic, and sliding mode.

The PV model in a current-mode controlled system uses the variable PV module voltage (V_{pv}) as its input ($I_{PV} = f(V_{PV})$). The PVE's output voltage (V_o) is electrically connected to the input of the PV model. The initial value of Vo is zero, and the photovoltaic (PV) model produces a reference current signal (I_{ref}) that is equivalent to the short circuit current (I_{sc}) at a specific irradiance (G) and temperature (T). In accordance with the I-V characteristic curve, the value of I_{ref} falls as V_o increases. Operational stability is attained when the voltage (V_o) and the output current (I_o) coincide with the output resistance (R_o) of the I-V curve. The PV model in a voltage-mode controlled system utilises the electric current (Ipv) of the PV module as its input ($V_{PV} = f(I_{PV})$). The PV emulator's output current (I_o) is connected to the electrical input of the PV model.

At first, the current (I_o) is zero, and the photovoltaic (PV) model produces a reference voltage signal (V_{ref}) that is equivalent to the open circuit voltage (V_{oc}) at specific values of grain size (G) and temperature (T). The value of V_{ref} drops as I_o increases, in accordance with the I-V curve. Operational stability is achieved when the values of V_o and I_o align with the point on the I-V curve that corresponds to R_o.

1.3 Part 3: Photovoltaic Models

Within the literature, several PV panel models can be categorized into two groups [5]: model-based types [24],[25], and model-based implementation schemes [26],[27],[28]. The interpolation model, derived from the I-V characteristic curve, achieves convergence with a single calculation, offering faster results. While the electrical circuit model requires complex theoretical parameters, the interpolation model only needs short circuit current and open circuit voltage. Despite the higher accuracy of the electrical circuit model, the 1D1R, single diode R_s model and 1D2R, single diode R_s /R_{sh} model, models are popular for their simplicity and accuracy. The single-diode model is suitable for amorphous silicon PV modules and high-power generation.

In contrast, the double diode model is more accurate under low irradiance and suitable for monocrystalline and polycrystalline silicon types, but it is a more complex mathematical model. For the second class, several approaches exist for implementing method-based model. The direct calculation method uses the 1D1R model for real-time computation, offering high accuracy but increasing computational load. The look-up table method reduces the processing burden by using pre-calculated I-V data, though it requires large memory and has lower adaptability. The piecewise linear model approximates the I-V curve with linear segments, improving dynamic performance but sacrificing accuracy. Moreover, employing AI techniques based on ANNs in PV models provides high accuracy, adaptability to various PV panels, and efficient real-time operation, making them particularly well-suited for testing and optimizing MPPT algorithms. [29],[30],[31],[32].

This paper investigates the development of a deep learning-based PV emulator that integrates an ANN with a DC-DC push-pull converter and a LQR with an integral action control strategy. Key contributions include:

- Employing an ANN to accurately emulate the

nonlinear characteristics of PV panels, generating a precise current reference for the emulator.
- Integrating LQR with integral action control.
- Using only one voltage sensor and estimating the current via a Luenberger observer, the emulator minimizes hardware requirements, enhancing efficiency compared to conventional control methods.

In light of the above, this work is organized as follows: Following the initial introduction, Section 2 provides a detailed description of the main parts of the proposed photovoltaic emulator, which includes the push-pull converter modeling, control strategy, and PV model. Section 3 presents the results of the simulated PVE to verify the performance of the suggested PVE. Finally, Section 4 presents the conclusion.

2 Proposed Photovoltaic Emulator

Fig 1 provides an overview of the proposed PVE, which includes three main parts:

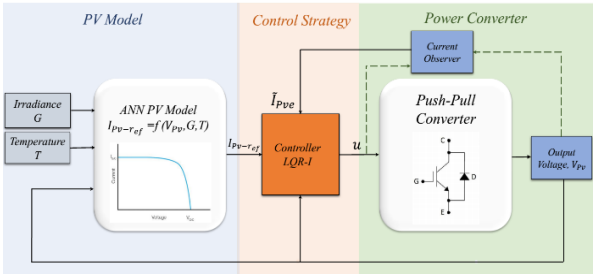

Fig.1 Proposed photovoltaic emulator schematic

1. *Power Converter:* This block primarily uses DC-DC converters, representing the power interface between the emulator and the load. They guarantee that the PVE output (voltage and current) matches the required characteristics of a PV panel.
2. *Control Strategy:* It ensures that the power converter accurately follows the reference current from the previous block with the fastest response time.
3. *Reference Trajectory Generation*: This part ensures the system mimics the behavior of a real photovoltaic system under various conditions by generating a reference current for the emulator to follow based on the actual output voltage. This is accomplished through a PV model that accurately reflects the characteristics and performance of the photovoltaic panel.

These three parts create a robust PVE that accurately simulates photovoltaic panels. The following subsections thoroughly explain each part.

2.1 Power Converter block: Description & Modelling

We rely on the isolated DC-DC push-pull converter for the power converter block in this part. It offers significant advantages for PV emulation, including electrical isolation for enhanced safety and protection, efficient handling of both low and high voltage levels, high efficiency, and a compact design suitable for high-power cases.

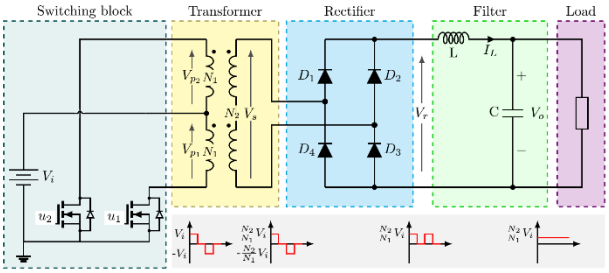

Fig. 2 Circuit diagram of push-pull converter

Figure 2 illustrates the circuit diagram of a push-pull converter, which mainly consists of four power stages:

- *Switching Block*: The switching block is the controlled component of the push-pull converter, responsible for alternating the input voltage between $+V_i$, 0, and $-V_i$ on the primary side of the transformer. This process generates a high-frequency AC voltage corresponding to the frequency of the pulse-width modulation (PWM) used to drive the two switches of this block, denoted as u_1 and u_2 in the circuit diagram.

- *High-frequency transformer:* This transformer converts the alternating voltage applied to its primary side into an alternating voltage on its secondary side, denoted as V_s., by either boosting or reducing it according to the turns ratio $\frac{N_2}{N_1}$.

- *Rectifier*: This power stage converts the AC voltage V_s to a rectified form, denoted V_r, with voltage levels of 0 and $\frac{N_2}{N_1}V_i$.

- *Filter*: It corresponds to a low-pass filter consisting of an inductor (L) and a capacitor (C) used to smooth out the high-frequency rectified voltage V_r. This block provides a constant DC output voltage to the load.

Equation (1) provides the average state-space representation of the push-pull converter [6]:

$$\begin{aligned} \dot{x} &= Ax + Bu \\ y &= Cx + Du \end{aligned} \tag{1}$$

With $x(t) = [I_L(t) \quad V_o(t)]^T$ represents the state vector where $I_L(t)$ is the inductor's current, $V_o(t)$ is the capacitor's voltage, and $u(t)$ denotes the system's input which corresponds to the average value of u_1 and u_2. The output $y(t)$ represents the measured state, which, in this work, we assume to be the output voltage $y(t)=V_o(t)$. The state, input, and output matrices are given by:

$$\mathbf{A} = \begin{bmatrix} 0 & -\frac{1}{L} \\ \frac{1}{C} & -\frac{1}{RC} \end{bmatrix}, \mathbf{B} = \begin{bmatrix} 2\frac{N_2}{N_1}\frac{V_i}{L} \\ 0 \end{bmatrix}, \mathbf{C} = [0 \quad 1]$$

The model described above will serve as the basis for the control design of the push-pull converter with the primary goal of ensuring that the converter operates at the operating point of the emulated PV panel.

2.2 Control Strategy: Analysis & Design

The push-pull converter is controlled in closed-loop current mode, where the PV model generates the reference current for the control strategy, equation (2), based on the converter's output voltage. The proposed control strategy is:

$$u(t) = -\mathbf{K}x(t) \quad (2)$$

- K represents a proportional action on the inductor's current and the capacitor's voltage. However, an integral action is required to track the reference current precisely. This can be guaranteed by incorporating additional state ξ(t), equation (3), to account for the integral of the error:

$$\xi(t) = \int_0^t I_{ref} - I_L(\tau)d\tau \quad (3)$$

Thus, the augmented model of the push-pull converter with the integral action is given by equation (4):

$$\begin{cases} \dot{x}_a(t) = \mathbf{A_a}x_a(t) + \mathbf{B_a}u(t) \\ y_a(t) = \mathbf{C_a}x_a(t) \end{cases} \quad (4)$$

with $x_a(t) = [x(t)^T \quad \xi(t)]^T$ and the following augmented matrices:

$$\mathbf{A_a} = \begin{bmatrix} \mathbf{A} & \mathbf{0}_{2\times1} \\ -\mathbf{C} & 0 \end{bmatrix}, \mathbf{B_a} = \begin{bmatrix} \mathbf{B} \\ 0 \end{bmatrix}, \mathbf{C_a} = \begin{bmatrix} 0 & 1 & 0 \\ 0 & 0 & 1 \end{bmatrix}$$

Now, the linear state feedback incorporates proportional and integral actions is given by equation (5):

$$u(t) = -\mathbf{K_a}x_a(t) \quad (5)$$

The literature provides various methods for designing linear feedback gain of the control law. These include pole placement [6], LQR [20],[21],[22], and robust control techniques. The next section aims to design an optimal state-feedback controller within the LQR framework.

2.2.1 Optimal State-Feedback Design

The LQR is a specific type of optimal control problem that aims to minimize a quadratic cost function. The latter is a combination of the state and control efforts over time. Equation (6), given the cost function is typically of the form:

$$J\big(u(t)\big) = \frac{1}{2}\int_0^\infty (x_a^T(t)\mathcal{Q}x_a(t) + u^T(t)\mathcal{R}u(t))dt \quad (6)$$

where $x_a(t)$ is the state vector, $u(t)$ is the control vector, and $Q \geq 0$ and $R > 0$ are weight matrices that penalize the state deviation and control effort, respectively. The solution to the LQR problem provides an optimal state feedback control law in the form of equation (5), where K_a is the optimal gain matrix that minimizes the cost function.

The optimal gain matrix is given by equation (7):

$$\mathbf{K}_a = \mathcal{R}^{-1}\mathbf{B}_a^T P \quad (7)$$

where $P \geq 0$ is the solution to the algebraic Riccati equation, (Eq.8):

$$\mathbf{A}_a^T P + P\mathbf{A}_a - P\mathbf{B}_a\mathcal{R}^{-1}\mathbf{B}_a P + \mathcal{Q} = 0 \quad (8)$$

Once the weight matrices are set, solving this equation provides the optimal gain.

2.2.2 Optimal Output-Feedback Design

The proposed control strategy at this level relies on both the output voltage and the inductor current measurements. As mentioned, the developed PVE depends solely on measuring the output voltage. To address this limitation, we propose using a Luenberger observer to estimate the system's state. The dynamic model of the observer is given by equation (9):

$$\begin{cases} \dot{\hat{x}}_a(t) = \mathbf{A_a}\hat{x}_a(t) + \mathbf{B_a}u(t) + \mathbf{L}_a\left(y_a(t) - \hat{y}_a(t)\right) \\ \hat{y}_a(t) = \mathbf{C_a}\hat{x}_a(t) \end{cases} \quad (9)$$

where $\hat{x}_a(t)$ is the estimated state, and $\mathbf{L_a}$ is the observer gain, chosen to ensure the estimation error remains stable.

The proposed control strategy for the push-pull converter is illustrated in Fig. 3 and is defined by equation (10):

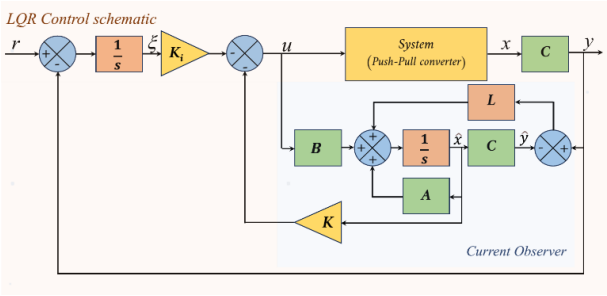

Fig.3 Block diagram of proposed control scheme

$$u(t) = -\mathbf{K_a}\hat{x}_a(t) = -(\boldsymbol{K_i}\xi(t) + \boldsymbol{K}\hat{x}_a(t)) \quad (10)$$

According to the separation principle, the design of the state feedback controller and the state estimator can be handled independently. Indeed, the estimation error dynamics is given by equation (11):

$$\dot{e}(t) = (\mathbf{A_a} - \mathbf{L_a}\boldsymbol{C_a})e(t) \quad (11)$$

with $e(t) = x_a(t) - \hat{x}_a(t)$ denote the estimation error. The system state equation under the proposed controller is given by equation (12):

$$\dot{x}_a(t) = \mathbf{A_a}x_a(t) - \mathbf{B_a}\mathbf{K_a}\hat{x}_a(t) \quad (12)$$

This can be rewritten by substituting $\hat{x}_a(t)$ with $x_a(t) - e(t)$ as presented in equation (13):

$$\dot{x}_a(t) = (\mathbf{A_a} - \mathbf{B_a}\mathbf{K_a})\hat{x}_a + \mathbf{B_a}\mathbf{K_a}e(t) \quad (13)$$

By regrouping the system in closed loop Eq. (13) with the estimation error Eq. (11), we obtain the following equation (14):

$$\begin{bmatrix} \dot{x}_a(t) \\ \dot{e}(t) \end{bmatrix} = \begin{bmatrix} \mathbf{A_a} - \mathbf{B_a}\mathbf{K_a} & \mathbf{B_a}\mathbf{K_a} \\ 0 & \mathbf{A_a} - \mathbf{L_a}\boldsymbol{C_a} \end{bmatrix} \begin{bmatrix} x_a(t) \\ e(t) \end{bmatrix} \quad (14)$$

Based on this, we can first address the LQR control design based on the actual system dynamics Eq. (4) and then focus on the design of the observer for estimating the states.

Remark: It should be noted that the control signals $u_1(t)$ and $u_2(t)$ for the push-pull converter are obtained using pulse width modulation (PWM). The average control $u(t)$ is compared to a triangular or sawtooth

carrier waveform to generate $u_1(t)$. For $u_2(t)$, a carrier waveform shifted by 180 degrees is used.

2.3 ANN Photovoltaic model

Integrating ANNs, especially deep learning, in PVEs has emerged as an advanced approach due to their ability to model nonlinear systems accurately. Early studies focused on developing ANN models that could accurately emulate the electrical behavior of PV modules. Researchers trained the models using multilayer perceptron (MLP) networks with backpropagation algorithms. These studies demonstrated that ANNs could effectively capture the nonlinear characteristics of PV systems [14]-[17], [23],[27].

This study specifically focuses on a type of ANN called a Feed-Forward Multilayer Perceptron (F-F MLP) because it can analyze large volumes of data for predictions with a multi-input, single-output (MISO) architecture [16],[17], [23].

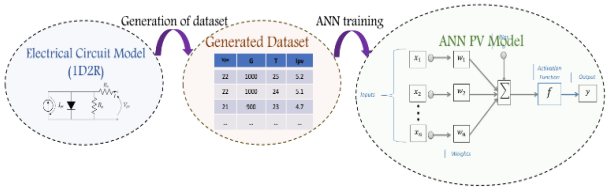

Fig.4 Training process of the PV-ANN

The dataset in the ANN's training process (Fig.4) was generated using the 1D2R electrical model of a PV panel with reference SW856 poly (Fig.5).

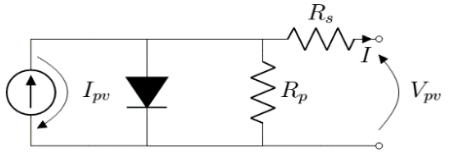

Fig.5 Electrical Circuit of the 1D2R PV model

Applying Kirchhoff's current law, the electrical PV 1D2R model is represented by the following equation (Eq.15):

$$I = I_{pv} - I_s\left(e^{\frac{V_{pv}+IR_s}{AV_T}} - 1\right) - \frac{V_{pv}+IR_s}{R_p} \qquad (15)$$

I_s: Is the reverse saturation current of the diode,
V_T: defined by: $V_T = \frac{K_B.T}{q}$,
K_B: Is the Boltzmann constant (1.38×10^{23}J/K),
T: Is the absolute temperature,
q: Is the basic electric charge (1.6×10^{-19}C).

The inputs to the ANN are irradiance (G), temperature (T), and measured voltage (V_o), while the output is the generated current under these conditions. A dataset of the ANN PV model is chosen with the following specifications as shown in Table 1.

Table 1 ANN PV model parameters

ANN Parameters	Values
Inputs	V_{pv} [V], G[w/m2] and T[°C]
Output	I_{pv} [A]
Architecture	Feed-Forward MLP
Learning rule	Backpropagation of errors
N=° hidden layers	4 (10 each)
Activation function	Sigmoid
Number of iterations	1000
Duration of training	495 seconds
Performance goal	$1x10^{-7}$
Learning Rate	0.05
Dataset	8e4

Figure 6 shows the regression analysis results of ANN PV model. The data represents the actual value, while the fitting represents the predicted values.

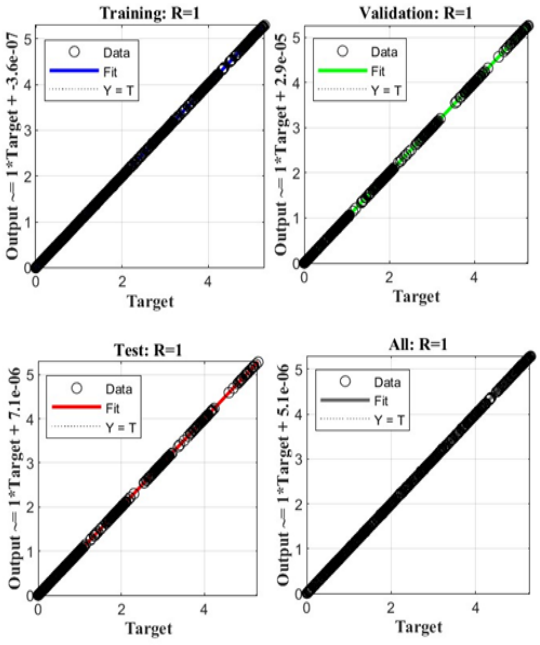

Fig.6 Regression analysis result of ANN PV model

2.3.1 Validation of the ANN PV model

In this sub-section, we compare the electrical PV model (SW85) with the obtained ANN PV model under different values of G and T. This comparison aims to validate the ANN PV model.

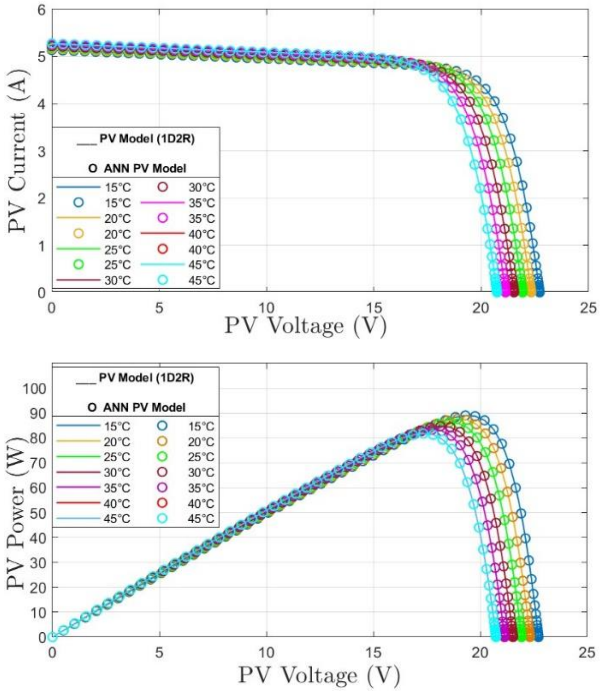

Fig.7 I-V and P-V curves under Temperature effects

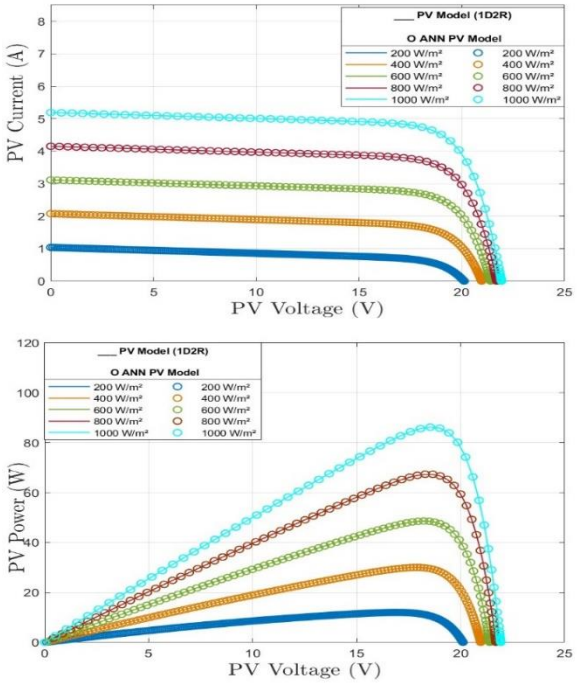

Fig.8 I-V and P-V curves under irradiance effects

Figure 7 shows the I-V and P-V curves of the SW 85 panel under varying temperature conditions. The comparison highlights the alignment between the electrical and the trained ANN PV models (represented by circles). A similar correspondence is observed in the curves under irradiance variation, as shown in Figure 8.

3 Simulation, Results, and Discussion

In this section, the proposed PVE (Fig.1), based on LQR control with a current observer, was simulated and tested under varying irradiance, temperature, and load conditions. To demonstrate the effectiveness of our proposed PVE, we conducted a comparative analysis between the LQR controller and the conventional PID control [6].

For our work, we used the following specifications:

- For Push-Pull converter parameters

  L=0.57H; C= 1.6µF and F=20 kHz.
- For LQR strategy: The following weight matrices are designed to ensure a fast response time with no overshoot in output current response:

$$Q = \begin{bmatrix} 1 & 0 & 0 \\ 0 & 0 & 0 \\ 0 & 0 & 1e6 \end{bmatrix}, R = 1.$$

Solving equation (8) yields the following optimal gain:

$$K = [2.06e2, -9.06e-4, -3.16e7]$$

- For the PID control design, we used a pole placement approach similar to the one described in [6]:

  K_p= 6, *Ki=2 and* K_d *=0.006.*

We used a pole placement approach for the observer design with the desired eigenvalues set as:

λ_1 = - 10e4, and λ_2 = - 50e4.

The resulting observer gain is:

$$L_a = [0.8e5 \;\; 5.913e5]$$

3.1 PVE Under Irradiance variation

To demonstrate the effectiveness of our PVE under Irradiance variation (Fig.9-a), the PV electrical model was compared as a reference to the proposed PVE controlled by LQR and PID, with constant load and temperature. In this scenario, the load was set to 5 Ω, with irradiance changing from 400 W/m² to 1000 W/m² at t=0.15s and from 1000 W/m² to 800 W/m² at t=0.35s.

Based on the analysis of Figure 9-b, 9-c, and 9-d, we conclude that the characteristics of the PV ANN emulator roughly correspond to the electrical PV model (reference) during abrupt variations in irradiance. This confirms the effective operation of the proposed ANN-based partial value extraction. Further observations indicate that the LQR controller outperforms the PID controller in terms of response time and steady-state error.

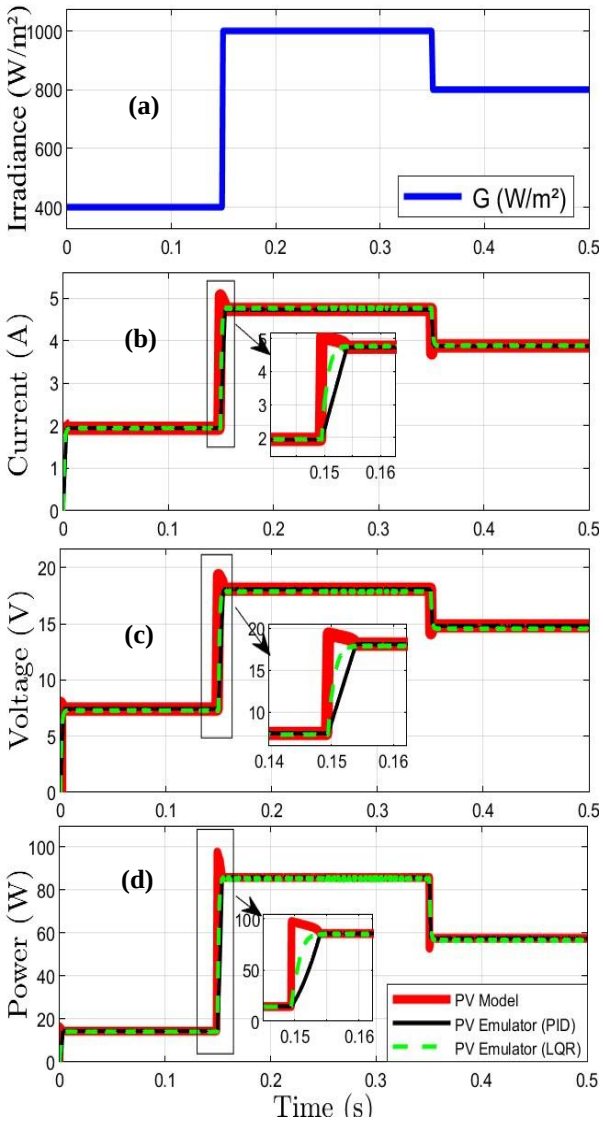

Fig.9 PV emulator under irradiance effect

3.2 PVE Under Temperature variation

In this subsection, the temperature was varied from 15 C to 30 C at 0.15s and from 30 C to 45 C at 0.35s, as shown in Fig.10-a.

Under sudden temperature changes, Figures 10-b,10-c, and 10-c show that the emulator behavior closely matches the predictions of the electrical model. This confirms the effectiveness of the proposed ANN-based PVE design with the LQR Controller compared to the conventional PID controller, in terms of steady-state error and response time.

3.3 PV emulator under Load variation

Another simulation has been made to compare the proposed PV emulator to the electrical PV model panel under load variation (Ramp), covering all load points from (I_{sc},*0*) to (*0*, V_{oc}).

As shown in Figures 11, the performance results indicate that the emulator's characteristics closely match those of the PV panel's electrical model at Standard Test Conditions (STC), confirming the effectiveness of our proposed emulator.

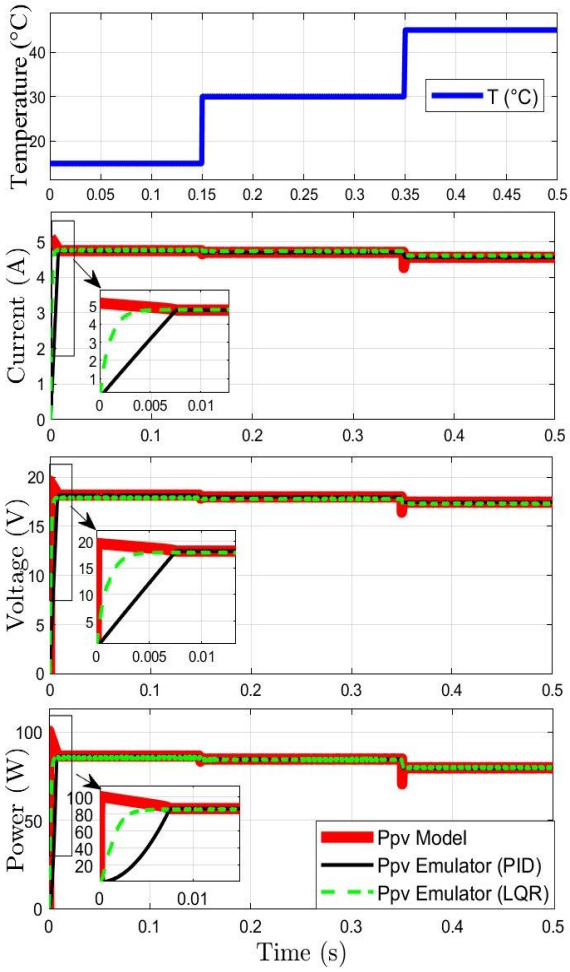

Fig.10 PV emulator under temperature effect

In comparing the two controllers, Table 2, the conventional PI controller achieved a response time of 7ms, while our proposed LQR with an observer significantly improved this to 2.5ms. This represents a considerable enhancement in response time with the LQR + observer approach reducing it by approximately 64.3%. These improvements are clearly highlighted in Fig. 10, which demonstrates the superior performance of the proposed approach in achieving faster system dynamics.

Table 2 Response time of various control strategies

Control strategy	PVE-PI [33]	PVE-FL [33]	PVE-SC [33]	PVE-PID (studied)	PVE-LQR (proposed)
At load 5Ω	3.5ms	3.0ms	3.5ms	7ms	2.5ms

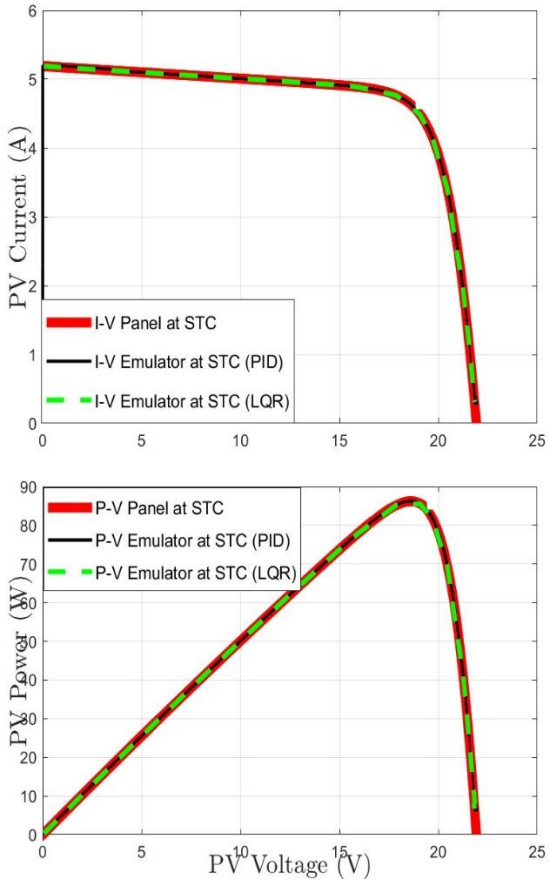

Fig.11 PV emulator under Load variation

4 Conclusion

In this study, we successfully developed and simulated a deep learning-based artificial neural network PVE using a push-pull converter controlled by a LQR strategy and incorporating a current observer. This work significantly contributes to the advancements of the PV emulator field, providing a robust and accurate tool for experimental investigations. The proposed ANN-based PVE demonstrates superior performance in terms of steady-state error and response time through reducing it by approximately 64.3% compared to conventional PID control technique.

Our results show that the deep learning-based ANN PV emulator precisely replicates the behavior of real PV panels under various irradiance, temperature, and load conditions, confirming its effectiveness and reliability. Using the LQR control strategy in conjunction with the current observer allows for precise current estimation with minimal hardware requirements, making it a highly efficient solution for PV emulation.

Overall, this paper provides valuable insights into the modeling and control of push-pull converters in PV emulation, offering a powerful platform for researchers and engineers to optimize the performance of power electronics systems connected to photovoltaic sources.

Conflict of Interest

The authors declare no conflict of interest.

Author Contributions

A. Hadjaissa and **M. Benmiloud**: Conceptualization, Methodology & Writing. **K. Ameur**: Formal Analysis & Review. **H.Bouchnak** and **M.Dimeh**: Software.

Each author has read and agreed to the published version of the manuscript.

References

[1] International Renewable Energy Agency (IRENA), Renewable Energy Statistics 2024, Abu Dhabi, 2024.

[2] Rystad Energy, "2024: Another Record Year for Solar PV Deployments, "https://www.rystadenergy.com/insights/2024-another-record-year-for-solar-pv-deployments.

[3] A. Allouhi, S. Rehman, M. S. Buker, Z. Said, "Up-to-date literature review on Solar PV systems: Technology progress, market status and R&D," Journal of Cleaner Production, vol. 362, 2022, Art. no. 132339.

[4] A. Aslam, N. Ahmed, S. A. Qureshi, M. Assadi, N. Ahmed, "Advances in Solar PV Systems; A Comprehensive Review of PV Performance, Influencing Factors, and Mitigation Techniques," Energies, vol. 15, no. 20, Art. no. 7595, 2022.

[5] R. Ayop, C. W. Tan, "A comprehensive review on photovoltaic emulator," Renewable and Sustainable Energy Reviews, vol. 80, pp. 430-452, 2017.

[6] M. Benmiloud, A. Hadjaissa, N. Abouchabana, K. Ameur, A. Benalia, A. Rabhi, "Design and Control of PV Emulator based on DC-DC Push-Pull Converter," in Proc. 2023 International Conference on Electrical Engineering and Advanced Technology (ICEEAT), Batna, Algeria, 2023, pp. 1-6.

[7] M. Chaker, A. El Houre, D. Yousfi, M. Kourchi, M. Ajaamoum, H. Idadoub, J. Bouchnaif, "Development of a PV emulator using SMPS converter and a model selection mechanism for characteristic generation," Solar Energy, vol. 239, 2022.

[8] P. S. Panuya, S. R. Salkuti, K. Mandal, M. Roy, S. C. Kim, "Design and Analysis of Digitally Operated PV Emulator with Resistive Load Using Newton–Raphson Method," in Energy and Environmental Aspects of Emerging Technologies for Smart Grid, Green Energy and Technology, 2024, pp. 1-11.

[9] S. Sharma, D. Joshi, "Reference Model Design, Control and Reliability Analysis of PV Emulator," in Renewable Energy Optimization, Planning and Control, Studies in Infrastructure and Control, 2023, pp. 1-12.

[10] Y. Kim, W. Lee, M. Pedram, N. Chang, "Dual-mode power regulator for photovoltaic module

emulation," Applied Energy, vol. 101, pp. 730–739, 2013.

[11] C. H. Balakishan, N. Sandeep, "Development of a microcontroller-based PV emulator with current controlled DC-DC buck converter," International Journal of Renewable Energy Research, vol. 4, no. 3, pp. 657-662, 2014.

[12] K. Bhise, N. Pragallapati, S. Thale, V. Agarwal, "Labview based emulation of photovoltaic array to study maximum power point tracking algorithms," in Proc. 2012 38th IEEE Photovoltaic Specialists Conference (PVSC), pp. 2961–2966, 2012.

[13] Z. Rasin, M. Rahman, M. Azri, M. H. Nizam, "Photovoltaic Emulator for Grid-connected Quasi-Z-Sorce Inverter," International Journal of Power Electronics and Drive Systems (IJPEDS), vol. 9, no. 4, pp. 1976-1988, 2018.

[14] R. G. Wandhare, V. Agarwal, "A low cost, light weight and accurate photovoltaic emulator," in Proc. 2011 37th IEEE Photovoltaic Specialists Conference, Seattle, WA, USA, 2011, pp. 1887-1892.

[15] M. H. MAHMUD, Y. ZHAO, "Sliding mode duty cycle control with current balancing algorithm for an interleaved buck converter-based PV source simulator," IET Power Electronics, vol. 11, no. 13, pp. 2117-2124, 2018.

[16] R. Raksha, S. K. Suryanarayana, "Modeling and analysis of 1.2 kW, 36–375 V, push–pull converter," Advances in Renewable Energy and Electric Vehicles, vol. 767, 2022.

[17] L. Yuan, T. L. Taewon, F. Z. Peng, D. L. Dichen, "A hybrid control strategy for photovoltaic simulator," in Proc. Twenty-Fourth Annual IEEE Applied Power Electronics Conference and Exposition (APEC), 2009, pp. 899–903.

[18] Ö. Duru, S. Zengin, M. Boztepe, "Design and implementation of programmable PV simulator," in Proc. 2016 International Symposium on Fundamentals of Electrical Engineering (ISFEE), 2016, pp. 1-6.

[19] R. Ayop, C. W. Tan, C. S. Lim, "The resistance comparison method using integral controller for photovoltaic emulator," International Journal of Power Electronics and Drive Systems, vol. 9, no. 2, pp. 820-828, 2018.

[20] A. Algaddafi, N. Brown, R. Gammon, S. Altuwayjiri, A. Rahil, S. Ali, "An Analogue Computation based Photovoltaic Emulator for realistic Inverter Testing," in Proc. 3rd International Conference on Energy Engineering, Faculty of Energy Engineering - Aswan University, Aswan, Egypt, Dec. 28-30, 2015, pp. 1-6.

[21] G. Martin-Segura, J. Lopez-Mestre, M. Teixido-Casas, A. Sudria-Andreu, "Development of a photovoltaic array emulator system based on a full-bridge structure," in Proc. 9th International Conference on Electrical Power Quality and Utilisation (EPQU), 2007, pp. 1-6.

[22] S. M. Azharuddin, M. Vysakh, H. V. Thakur, N. B. Nishant, T. S. Babu, K. Muralidhar, et al., "A near accurate solar PV emulator using dSPACE controller for real-time control," Energy Procedia, vol. 54, pp. 2640–2648, 2014.

[23] A. Koran, K. Sano, R. Y. Rae-Young, J. S. Jih-Sheng, "Design of a photovoltaic simulator with a novel reference signal generator and two-stage LC output filter," IEEE Transactions on Power Electronics, vol. 25, no. 5, pp. 1331–1338, 2010.

[24] G. Ciulla, V. Lo Brano, V. Di Dio, G. Cipriani, "A comparison of different one-diode models for the representation of I-V characteristic of a PV cell," Renewable and Sustainable Energy Reviews, vol. 32, pp. 684-696, 2014.

[25] M. S. Rasheed, S. Shihab, "Modelling and Parameter Extraction of PV Cell Using Single-Diode Model," Advanced Energy Conversion Materials, vol. 1, no. 2, pp. 96-104, 2020.

[26] S. Gadelovits, M. Sitbon, A. Kuperman, "Rapid prototyping of a low-cost solar array simulator using an off-the-shelf DC power supply," IEEE Transactions on Power Electronics, vol. 29, no. 10, pp. 5278–5284, 2014.

[27] S. Jin, D. Zhang, "A simple control method of open-circuit voltage for the FPGA based solar array simulator," in Proc. IEEE International Conference on Power and Renewable Energy (ICPRE), 2016, pp. 209–216.

[28] M. T. Iqbal, M. Tariq, M. S. U. Khan, "Fuzzy logic control of buck converter for photovoltaic emulator," in Proc. 4th International Conference on Development in Renewable Energy Technology (ICDRET), 2016, pp. 1–6.

[29] F. Gomez-Castaneda, G. M. Tornez-Xavier, L. M. Flores-Nava, O. Arellano-Cardenas, J. A. Moreno-Cadenas, "Photovoltaic panel emulator in FPGA technology using ANFIS approach," in Proc. 11th International Conference on Electrical Engineering, Computing Science and Automatic Control (CCE), 2014, pp. 1-6.

[30] E. Karatepe, M. Boztepe, M. Colak, "Neural network based solar cell model," Energy Conversion and Management, vol. 47, no. 9, pp. 1159–1178, 2006.

[31] K. Saraswathi, K. Thankanadar, A. Parassuram, V. Swaminathan, G. Periasamy, S. Somasundaram, "An Artificial Neural Network-Based Comprehensive Solar Photovoltaic Emulator," International Journal of Photoenergy, vol. 2022, Article ID 4741428, 2022.

[32] S. Sharma and D. Joshi, "PV Emulator Model Design Using AI-Based Controllers," in Proc. 3rd International Conference on Computing Informatics and

Networks, A. Abraham, O. Castillo, and D. Virmani, Eds., vol. 167, Lecture Notes in Networks and Systems. Springer, Singapore, 2021, pp. 1-12.

[33] Ayop, R., Wei Tan, C. and Lawan Bukar, A., Simple and fast computation photovoltaic emulator using shift controller. IET Renewable Power Generation, (2020) 14: 2017-2026. https://doi.org/10.1049/iet-rpg.2019.1504.

Dr. Aboubakeur Hadjaissa is an associate professor at the Department of Electronics, University of Laghouat from 2012. He holds a Doctorate in Science from National Polytechnic School, Algiers, in 2016, with expertise in renewable energy systems, particularly photovoltaic and hybrid energy systems. His research focuses on power electronics, control systems, and optimization techniques.

Dr. Benmiloud Mohammed is an Assistant Professor at the Department of Electronics, University of Amar Telidji, Laghouat, Algeria. He earned his Ph.D. in Control Engineering in 2017 under the joint supervision of the University of Laghouat and the Université Polytechnique Hauts-de-France. Following his doctorate, he completed a postdoctoral fellowship at École Centrale de Nantes in France from 2017 to 2018, and later served as a Research Associate at the University of Cambridge in the UK from 2018 to 2019. His research focuses on advanced control systems, nonlinear dynamics, renewable energy technologies, power electronics, and microgrids.

Khaled AMEUR received the Engineer's degree in Electronics from Laghouat University in 2005, the Magister's degree in Instrumentation from the University of Science and Technology Houari Boumediene, Algiers, in 2009 and the PHD in Electrical engineering from Laghouat University in 2018. He is currently an associate professor at the department of Electronics in Laghouat University. From 2011 to 2015, Khaled taught courses on photovoltaic systems, MATLAB programming, power electronics, and analog electronics. He is currently teaching advanced power electronics and applied electronics at Laghouat University. His research interests include renewable energies, EV chargers, power electronics, control systems, and battery management, where he continues to contribute to advancing these fields.

Halima BOUCHNAK earned her Bachelor's degree in Automation from the University of Laghouat in 2022 and completed her Master's degree in Automation and Industrial Computing at the University of Laghouat, Algeria, in 2024. Her research focuses on control systems and photovoltaic systems.

Maria DIMEH earned her Bachelor's degree in Electronics from the University of Laghouat in 2022 and completed her Master's degree in Automation and Industrial Computing at the University of Laghouat, Algeria, in 2024. Her research focuses on control systems and photovoltaic systems.